

Research Article

Pressure Effect on Thermodynamic Quantities for the Solid-Liquid Phase Transition in n-tridecane, n-hexadecane and n-octadecane

¹O. Tari^{ORCID}, ^{2*}H. Yurtseven^{ORCID}

¹ Department of Electrical and Electronics Engineering, Istanbul Arel University, 34537 Büyükçekmece, Istanbul-TURKEY

² Department of Computer Engineering, Baskent University, 06790 Ankara – TURKEY
E-mail: ^{2*}hamit@metu.edu.tr

Received 4 August 2023, Revised 11 October 2023, Accepted 23 October 2023

Abstract

The pressure effect is investigated regarding the solid – liquid equilibria (SLE) in n-alkanes. Using the Landau phenomenological model, the pressure dependences of the thermodynamic functions are predicted and the phase diagrams are constructed for the solid – liquid transitions in the binary mixtures of n-alkanes. The experimental data from the literature are used for the phase diagrams in the mixtures.

Our fits for the phase diagrams are reasonably good. Regarding the cubic dependence of the concentration ($T - X$, $P - X$) and the linear dependence of the pressure ($P - T$) on the temperature, our results show that the n-tridecane is distinguished from the other mixtures due to its lowest freezing temperature ($T_1 = 291.08$ K) and correspondingly higher concentration ($x_1 = 0.1982$). It is found that the divergence behaviour of the heat capacity (C) with the critical exponent $1/2$ from the extended mean field model is in particular more apparent at the room temperature (293.15 K) at various pressures for the solid – liquid transition. This is accompanied with the pressure dependences of the order parameter, susceptibility, entropy and enthalpy for those mixtures as studied here.

Keywords: Phase diagrams; thermodynamic quantities; Landau model; n-tridecane; n-hexadecane; n-octadecane.

1. Introduction

Normal alkanes (n-alkanes) and their mixtures have been studied extensively over the years. In particular, studies on the phase boundary between the homogenous liquid phase and the two-phase liquid – solid phase domain, have been reported [1, 2]. Also, their specific rotator phases and intricate phase transition behavior have been the subject of various studies [3]. A number of studies [4-7] have been devoted to describe the structure and the phase transitions of the rotator phases, as indicated previously [3]. Small linear alkanes and their cyclic counterparts have been examined by molecular dynamic simulations and, thermodynamic, structural and dynamic behavior of liquids have been studied [8]. Among various mixtures of n-alkanes, confined crystallization behaviours of binary even-even normal alkane (n-alkane) mixtures of n-octadecane (n-C₁₈H₃₈) and n-eicosane (n-C₂₀H₄₂) have also been studied [9]. Melting curves of pure heavy paraffins were measured in earlier studies [10-13]. However, the pressure effect on the solid-liquid equilibria of complex mixtures of long-chain alkanes has not been investigated in those earlier studies. Later, a set of measurements were carried out on tridecane for the pressures up to 100 MPa in several synthetic mixtures, n-paraffins, ranging from n-C₁₃ to n-C₂₄ with various number of components [14]. The influence of pressure on the rotator phases was also studied within the Landau mean field theory [3]. Experimental phase diagram of the alkane system, namely, dodecane-tridecane was evaluated to study phase

change materials (PCMs) for freezing applications [13]. Also, experimental measurements and thermodynamic modeling for the binary mixtures of n-C₁₁H₂₄ have been carried out [15].

The pressure dependence of both the lattice distortion and the order of the rotator transitions has been discussed within the Landau theory in some details [16]. Also, rotator phases of n-heptane have been studied by Raman scattering and X-ray diffraction under high pressures [17]. For such a system, a liquid to solid transition has been predicted by the high pressure molecular dynamic (MD) simulations [18]. Rotator phases in alkane systems regarding bulk, surface layers and micro/nano confinements have been reviewed [19]. Experimentally, $T - X$ data at various pressures for binary mixtures of $(1 - x)n - C_{14} + xn - C_{16}$ (tetradecane + hexadecane) have been obtained [20, 21]. The temperature – dependent Raman spectra have been obtained for tetradecane, pentadecane and hexadecane [22]. $T - X$ phase diagram and the thermodynamic quantities were also calculated for this binary mixture [23-26] and for the n-tridecane [27] close to the liquid - solid phase transition using Landau phenomenological model in our recent studies.

Heat capacities of n-heneicosane and n-decosane have been measured and the thermodynamic properties such as entropy and enthalpy were calculated [28]. Also, by means of the molecular dynamic simulations, solid – liquid and solid – solid phase transitions in alkanes have been studied [29]. Regarding the heat capacity of the rotator phases of

alkanes, effect of silica nanoparticles has been studied theoretically by combining Flory-Huggins free energy (isotropic mixing) and Landau free energy [30]. Also, rotator phases in hexadecane have been studied experimentally [31].

Regarding the phase diagrams of binary mixtures of n-alkanes at high pressures, $T - X$ and $P - X$ (at constant temperatures) phase diagrams for n-tridecane + n-hexane were obtained from the experimental measurements [32]. Also, $T - X$ phase diagrams of n-alkane+cyclohexane where n-alkanes are n-hexadecane, n-octadecane and n-eicosane, were obtained at 300 MPa experimentally and the (solid + liquid) equilibria (SLE) of those n-alkanes were modelled [32]. The pressure effect on the physical and chemical properties of n-alkanes, has not been studied fully whereas the temperature effect on those properties was studied in a large scale as given in the literature. Mainly, the experimental measurements such as on tridecane up to 100 MPa [14] and the phase diagrams of n-alkanes [32], have been reported, as stated above. Theoretically, studies regarding the pressure effect on the phase diagrams and also on the thermodynamic functions, are relatively limited, as reported in the literature. Using the Landau mean field theory, in particular, the influence of the pressure has been studied for the rotator phases in n-alkanes [3, 16], as also stated above. From this point of view, the experimental measurements for the phase diagrams and for the thermodynamic properties at various pressures, require the theoretical analysis using some models. This present study by using the Landau phenomenological model, aims to fulfill this gap to describe the pressure effect on the thermodynamic properties for the solid – liquid equilibria in the binary mixtures (n-tridecane, n-hexadecane and n-octadecane). In order to describe the solid – liquid equilibria in n-alkanes, the thermodynamic properties have been studied mostly at various temperatures, as reported in the literature. Regarding our previous studies, $T - X$ phase diagram and also under high pressure for tetradecane + hexadecane [23, 26], $T - n$ (number of carbons) phase diagram of n-alkanes [24], and for n-tridecane [27] have been reported, as mentioned above. Additionally, the thermodynamic quantities have been calculated as a function of temperature [23, 26, 27] using Landau phenomenological model. However, the effect of the pressure on the transition mechanism for the solid – liquid equilibria, as studied for the phase diagrams of n-alkanes in our previous publications [25, 27], should also be studied for the thermodynamic quantities in those binary mixtures. From this point of view, the present study differs from the already published works in the sense that it uses the Landau phenomenological model and also it differs from our previous works [23-27] since in this study, thermodynamic functions are calculated as a function of pressure for the binary mixtures studied.

In this study, the $T - X$ phase diagrams (n-alkanes + n-cyclohexane) at 300 MPa, $P - X$ phase diagrams (n-alkanes + n-hexane) at constant temperatures and $P - T$ phase diagrams (n-alkanes + n-hexane) at constant concentrations (mole fractions) were calculated using the experimental data [32]. For this calculation, the phase line equations which were extracted from the free energy, are fitted to the experimental data [32]. As an original work, the $T - X$ phase diagram is represented by a single polynomial curve for n-hexadecane, n-octadecane and n-eicosane, whereas for n-tridecane the $T - X$ relation is obtained as linear from the Landau phenomenological model.

It has been shown in our previous study [26] that the extended mean field model can describe adequately the critical behavior of the heat capacity C and the other thermodynamic quantities as a function of temperature for the solid – liquid transition in the tetradecane + hexadecane. As an original study, the present paper aims to describe the solid – liquid equilibria in the binary mixtures of n-tridecane, n-hexadecane and n-octadecane by calculating the pressure dependence of the heat capacity C and also to predict the order parameter, susceptibility, entropy and enthalpy as a function of pressure at constant temperature by means of the extended mean field model. So that the pressure dependences of the order parameter, susceptibility and the thermodynamic quantities such as heat capacity, entropy and enthalpy were predicted for the solid-liquid transitions in these binary mixtures studied. Our motivation in the present study is to describe the liquid-solid equilibria and to investigate the phase change mechanism of the materials consisting of n-alkanes mixtures.

The present work illustrates the possibility of describing theoretically temperature – concentration – pressure phase diagrams and the pressure – induced phase changes in n-alkanes. This would lead to the fundamental understanding of the structural, physical and chemical properties of n-alkane molecules.

2. Theory

The pressure effect on the solid – liquid transition in n-alkanes can be investigated by the Landau mean field theory. Since this theory is applicable to the experimental measurements, by analyzing the observed data for the phase diagrams and the thermodynamic quantities, the first order solid – liquid equilibria (SLE) can be studied. This is done by expanding the free energy in terms of the order parameter. By obtaining the phase line equation from the free energy, the $T - X$, $P - X$ and $P - T$ phase diagrams can be constructed for n-alkanes on the basis of the experimental data. By means of the phase diagrams, the pressure dependence of the thermodynamic quantities can be predicted close to the solid – liquid transition in those mixtures. In this study, the pressure effect, in particular, on the mixtures of n-alkanes (1) + n-hexane (2), where n-alkanes (1) are n-tridecane (1), n-hexadecane (1) and n – octadecane (1) is investigated using the experimental data [32].

Various forms of the free energy in terms of the order parameters have been given in the literature. Thermodynamic model for a Landau model for the melting transition has been given [33]. The extended mean field model [34] has been introduced, mainly for the liquid crystals [35]. The coupled order parameters in the free energy expansion have been studied within the Landau phenomenological model [3, 16, 36, 37]. The free energy expansion with the coupled order parameters describing the solid – liquid transition in n-alkanes have been given in our recent studies [23 - 27]. In particular, the form of the free energy as given by the extended mean field theory [34], has been used in this study for the free energy of the solid phase (F_s) for the solid – liquid equilibria in terms of the order parameter η as

$$F_s = a_2\eta^2 + a_4\eta^4 + a_6\eta^6 \quad (1)$$

where the coefficients are assumed to depend on the temperature, pressure and concentration, in general. For the

solid – liquid equilibria, we have the first order condition that [38]

$$F_s = F_L = 0 \quad (2)$$

by considering the fact that in the liquid phase there is no ordering ($F_L = 0$). For the SLE, the coefficients are $a_2 > 0$, $a_4 < 0$ and $a_6 > 0$ for the first order transition as defined by the Landau mean field theory. Minimizing the free energy with respect to the order parameter ($\partial F_s / \partial \eta = 0$) as performed in our earlier studies [23 - 27], gives

$$a_2 + 2a_4\eta^2 + 3a_6\eta^4 = 0 \quad (3)$$

Using the first order condition (Eq. (2)), the order parameter can be written as

$$\eta^2 = -a_4/2a_6 = a_2/4a_4 \quad (4)$$

as also obtained previously [23, 26]. Substituting Eq. (4) into Eq. (1) and using Eq. (2), the phase line equation is obtained as

$$a_2a_6 = -2a_4^2 \quad (5)$$

for the SLE of the mixtures (n-alkanes) [23, 25, 26].

Thermodynamic quantities can also be calculated as a function of pressure for the SLE of the n-alkanes. As the order parameter η (Eq. (4)) was obtained, the inverse susceptibility using the definition

$$\chi_\eta^{-1} = \partial^2 F_s / \partial \eta^2 \quad (6)$$

can be predicted from the free energy F_s (Eq. (1)) as

$$F = a_2\psi^2 + a_3\psi^3 + a_4\psi^4 \quad (7)$$

similar to the calculation of χ_η^{-1} [23, 26].

For the thermodynamic quantities such as the heat capacity (C), entropy (S) and the enthalpy (H), the extended mean field model [34] is employed as applied to predict the heat capacity of the smectic A – smectic C (AC) transition in liquid crystals [35]. According to this model, the temperature dependence of the heat capacity is given by [35]

$$C = C_o T (T_1 - T)^{-1/2} \quad (8)$$

where T_1 denotes the melting temperature and C_o is a constant for the SLE in n-alkanes. This gives rise to the entropy difference $\Delta S = S - S_o$ from the definition $C/T = \partial S / \partial T$ as

$$\Delta S = \partial F / \partial T = -2C_o (T_1 - T)^{1/2} \quad (9)$$

where S_o is the entropy at the melting temperature ($T = T_1$). The enthalpy difference $\Delta H = H - H_o$ can also be obtained from the definition $C = \partial H / \partial T$ as

$$\Delta H = -C_o T (T_1 - T)^{1/2} \quad (10)$$

Similar calculation of the entropy (Eq. (9)) and the enthalpy (Eq. (10)) has been performed in our recent studies [23, 26]. In the derivation of Eq. (10), the $(T_1 - T)^{3/2}$ term is neglected as compared to the $(T_1 - T)^{1/2}$ term which is

dominant for the critical behavior of the enthalpy close to the solid – liquid transition in n-alkanes.

On the basis of the extended mean field model [35], the temperature dependence of the order parameter ψ (or η) can be obtained from the heat capacity as

$$\psi^2 = \int_T^{T_1} (C/T) dT \quad (11)$$

or by means of Eq. (8), ψ can be expressed as

$$\psi = \psi_0 (T_1 - T)^\phi \quad (12)$$

with the critical exponent $\phi = 1/4$ and the amplitude $\psi_0 = (2C_o)^{1/2}$.

3. Calculations and Results

The temperature, pressure and the concentration dependences of the phase line equation and the thermodynamic quantities studied, can be obtained by means of those dependences of the coefficients a_2 , a_4 and a_6 (Eq. (1)). By assuming that

$$a_2 = a_{20}(T - T_1) + a_{21}(P - P_1) \quad (13)$$

and

$$a_4 = a_{40} + a_{41}(x - x_1) + a_{42}(x - x_1)^2 \quad (14)$$

where T_1 , P_1 and x_1 represent the melting temperature, pressure and the mole fraction (concentration), respectively.

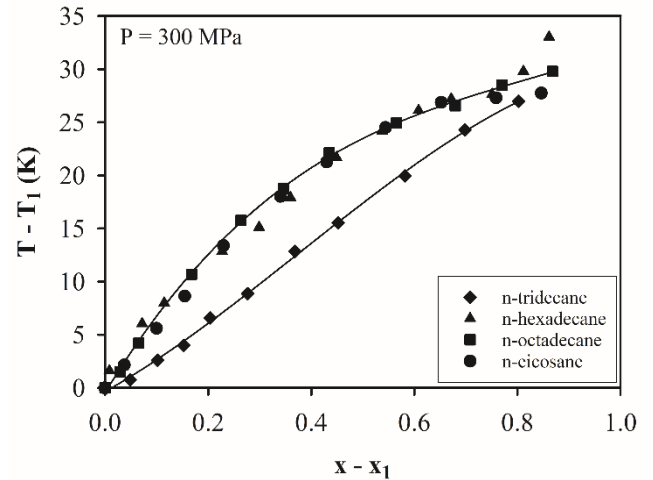


Figure 1. T - X phase diagrams calculated according to the phase line equation (Eq. (15)) which was fitted to the experimental data [32] for the solid – liquid transition of the mixtures of n-alkane (1) + n-cyclohexane (2) at $P=300$ MPa. Experimental data (within the range of temperatures) are also shown in the figure.

The coefficient a_6 in Eq (1) was considered as a constant ($a_6 = a_{60}$), independent of temperature, pressure and concentration in our treatment. The phase line equation (Eq. (5)) can then be obtained as follows:

$$T - T_1 = \alpha_0 + \alpha_1(x - x_1) + \alpha_2(x - x_1)^2 + \alpha_3(x - x_1)^3 + \alpha_4(P - P_1) \quad (15)$$

where α_0 , α_1 , α_2 , α_3 and α_4 are all constants. Those coefficients are defined as

$$\begin{aligned}
\alpha_0 &= -\frac{2a_{40}^2}{c} \\
\alpha_1 &= -4a_{40}a_{41}/c \\
\alpha_2 &= -2(a_{41}^2 + 2a_{40}a_{42})/c \\
\alpha_3 &= -4a_{41}a_{42}/c \\
\alpha_4 &= -a_{21}/a_{20}
\end{aligned}
\tag{16}$$

with the definition of $c = a_{20}a_{60}$.

In this study, the $T - X$ phase diagram was calculated for the mixtures of n-alkane (1) + cyclohexane (2) with the n-alkanes : n-tridecane (1), n-hexadecane (1), n-octadecane (1) and n-eicosane (1) at the pressure 300 MPa according to the $T - X$ phase line equation (Eq. (15)) from the Landau phenomenological model. Eq. (15) at $P = P_1 = 300$ MPa, was fitted to the experimental data [32] and the $T - X$ plots were obtained as shown in Fig. 1 for all those mixtures. Coefficients which were determined from the fits and the experimental [32] freezing temperatures T_1 with the mole fraction x_1 of n-alkanes considered, are given in Table 1.

In order to investigate the pressure effect on the solid – liquid transitions in n-alkane mixtures, $P - X$ phase diagrams at constant temperatures were constructed according to Eq. (15). For this study, Eq. (15) was fitted to the experimental data [32] at $T = T_1$ and the $P - X$ phase diagrams were obtained. Fig. 2 gives the $P - X$ phase diagrams at constant temperatures indicated for the composition x_1 for the a) n-tridecane (1) + n-hexane (2), b) n-hexadecane (1) + n-hexane (2) and c) n-octadecane (1) + n-hexane (2) systems. Coefficients determined, are given in Tables (2-4), respectively.

$P - T$ phase diagrams at constant mole fractions were also established for the solid – liquid equilibria (SLE) in the binary mixture of n-tridecane (1) + n-hexane (2) by Eq. (15) using the experimental data [32]. By choosing constant mole fractions at $x = x_1$ (Eq. (15)), the $P - T$ phase diagrams were predicted in this system, as plotted in Fig. 3(a). Values of the coefficients (Eq. (15)) which were determined for the n-tridecane (1) + n-hexane (2), are given in Table 5. Similarly, the $P - T$ phase diagrams were predicted for the systems of n-hexadecane (1) + n-hexane (2) and n-octadecane (1) + n-hexane (2) by fitting Eq. (15) to the experimental data [32] at constant mole fractions as shown in Figs. 3b and 3c, respectively, for the solid – liquid transition in those mixtures. Coefficients determined, are also given in Table 5.

Our assumption for the temperature and pressure dependence of the coefficient a_2 (Eq. (13)) represents the simplest form for the linear $T - P$ relation in the liquid – solid transition of the binary mixtures considering Eq. (5) where $a_6 = a_{60}$ as a constant. This is in accordance with the phase line equation (Eq. (5)) since we also assumed the coefficient a_4 which depends only on the concentration x (Eq. (14)). At the transition pressure ($P = P_1$), the temperature dependence of a_2 is simply $a_2 = a_{20}(T - T_1)$ which is the usual temperature dependence of the squared term in the order parameter (η^2) according to Eq. (1) in the Landau theory. From this point of view, a linear $T - P$ relation can be established in the phase diagram for the liquid – solid transition by assuming a_2 as in (Eq. (13)).

It was also assumed the quadratic dependence of the coefficient a_4 on the concentration (Eq. (14)). This assumption is also in accordance with the $T - P$ relation (Eq. 3.1) at the concentration of the first component in the binary mixture ($x = x_1$) in Eq. (14) regarding the phase line

equation (Eq. (5)) by ignoring the fourth order term in the concentration, $(x - x_1)^4$. As a result of this, cubic dependence of the temperature on the concentration (Eq. 3.3) was obtained for the $T - X$ phase diagram ($P = P_1$).

Our assumptions for the coefficients a_2 (Eq. (13)) and a_4 (Eq. (14)) can be demonstrated with the experimental measurements [32] on the n-alkanes studied here for a linear variation of pressure with the temperature at $x = x_1$ ($P - T$ phase diagrams), as shown in Fig. 3.

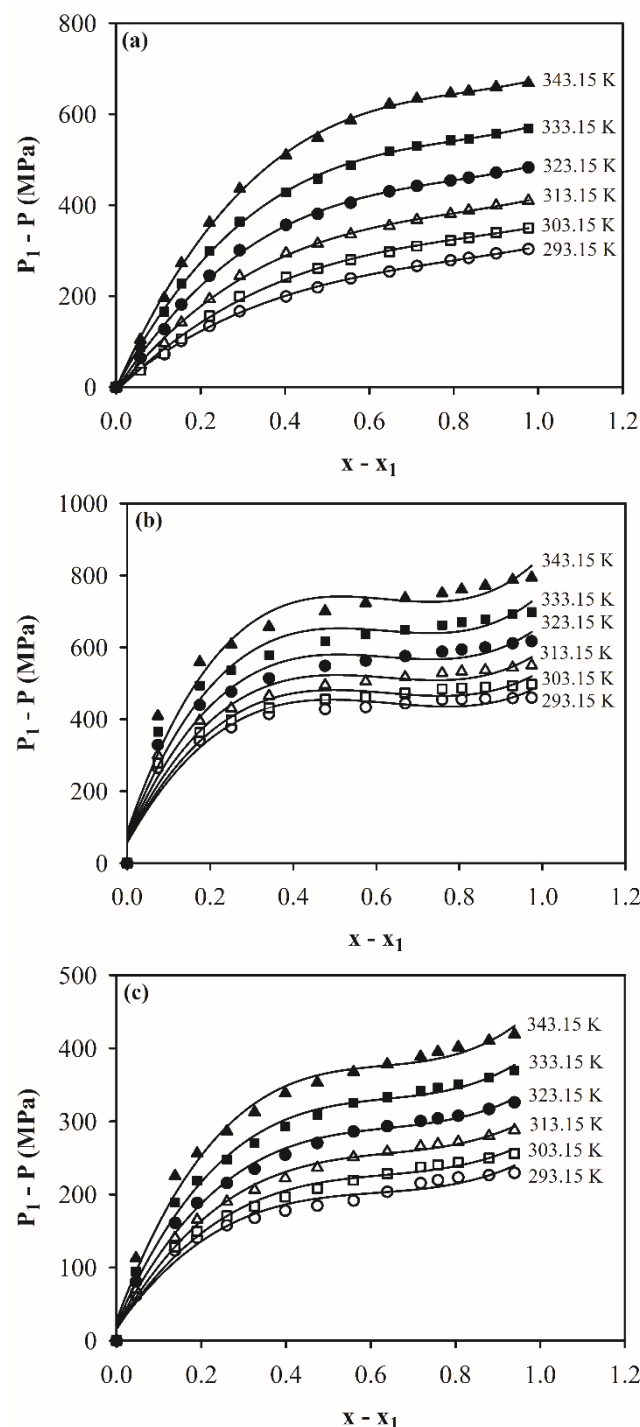


Figure 2. $P - X$ phase diagram calculated according to the phase line equation (Eq. (15)) which was fitted to the experimental data [32] for the solid – liquid transition of the mixtures a) n-tridecane (1) + n-hexane (2) b) n-hexadecane (1) + n-hexane (2) c) n-octadecane (1) + n-hexane (2) at constant temperatures indicated. Experimental data are also shown in the figure.

Table 1. Values of the coefficients determined for the solid – liquid transitions in the mixtures indicated according to the $T - X$ phase line equation (Eq. (15)) at $P=300$ MPa by using the experimental data [32]. Values of the freezing temperatures T_1 (within the range of experimental temperature) and the mole fraction x_1 of n-alkanes are also given.

T - X (Eq. 3.3)	n-tridecane (1) + cyclohexane (2)	n-hexadecane (1) + cyclohexane (2)	n-octadecane (1) + cyclohexane (2)	n-eicosane (1) + cyclohexane (2)
T_1 (K)	291.08	318.07	328.97	337.72
x_1	0.1982	0.1406	0.1340	0.1553
α_0 (K)	-0.3488	0.7428	-0.4523	-0.2115
α_1 (K)	27.22	67.44	79.78	64.58
α_2 (K)	29.75	-63.26	-80.17	-30.04
α_3 (K)	-26.49	31.39	32.65	-8.82

Table 2. Values of the coefficients determined for the solid – liquid transitions in the n-tridecane (1) + n-hexane (2) systems at constant temperatures indicated by using the experimental data [32] according to Eq. (15).

T (K)	293.15	303.15	313.15	323.15	333.15	343.15
P_1 (MPa)	436.17	547	675.17	820.69	983.54	1163.74
$(-\alpha_0/\alpha_4)$ (MPa)	0.246	9.639	8.609	7.282	1.801	2.236
$(\alpha_1/\alpha_4) \times 10^3$ (MPa)	0.752	0.925	1.158	1.446	1.740	2.070
$(-\alpha_2/\alpha_4) \times 10^3$ (MPa)	0.752	0.922	1.246	1.632	1.987	2.323
$(\alpha_3/\alpha_4) \times 10^2$ (MPa)	3.086	3.597	5.117	6.832	8.261	9.317

Table 3. Values of the coefficients determined for the solid – liquid transitions in the n-hexadecane (1) + n-hexane (2) systems at constant temperatures indicated by using the experimental data [32] according to Eq. (15).

T (K)	293.15	303.15	313.15	323.15	333.15	343.15
P_1 (MPa)	469.45	548.68	645.85	760.97	894.02	1045.01
(α_0/α_4) (MPa)	56.85	60.08	64.78	70.62	77.55	85.55
$(\alpha_1/\alpha_4) \times 10^3$ (MPa)	2.056	2.166	2.346	2.600	2.930	3.335
$(-\alpha_2/\alpha_4) \times 10^3$ (MPa)	3.424	3.603	3.897	4.319	4.862	5.529
$(\alpha_3/\alpha_4) \times 10^3$ (MPa)	1.808	1.913	2.078	2.313	2.606	2.963

Table 4. Values of the coefficients determined for the solid – liquid transitions in the n-tridecane (1) + n-hexane (2) systems at constant temperatures indicated by using the experimental data [32] according to Eq. (15).

T (K)	293.15	303.15	313.15	323.15	333.15	343.15
P_1 (MPa)	238.60	305.71	383.16	470.94	569.05	677.49
(α_0/α_4) (MPa)	17.47	15.85	16.10	18.22	22.19	28.02
$(\alpha_1/\alpha_4) \times 10^3$ (MPa)	0.818	0.892	1.002	1.149	1.333	1.553
$(-\alpha_2/\alpha_4) \times 10^3$ (MPa)	1.262	1.322	1.464	1.689	1.995	2.384
$(\alpha_3/\alpha_4) \times 10^2$ (MPa)	6.849	6.948	7.577	8.734	1.042	1.264

$T - X$ (at $P = P_1$) phase diagrams (linear and quadratic fits are also possible) (Fig. 1) and $P - X$ (at $T = T_1$) phase diagrams (Fig. 2) were also based on the experimental measurements [32].

In our previous studies [23, 25, 26] linear dependence of the coefficient a_2 on the temperature and concentration, and the quadratic dependence of a_4 on the concentration, have been assumed to describe the observed phase diagrams of tetradecane + hexadecane within the Landau phenomenological model. Recently, those dependences have

also been assumed for the solid – liquid equilibria in n-tridecane [27].

As studied for the $P - X$ and $P - T$ phase diagrams, the pressure effect was also investigated on the thermodynamic quantities for the solid – liquid phase transition in the mixtures considered in this study. For that purpose, the order parameter, susceptibility and the thermodynamic quantities of heat capacity, entropy and enthalpy were predicted as a function of pressure at constant temperatures by means of the Landau phenomenological model on the basis of the $P - X$ and $P - T$ phase diagrams for the mixtures studied here. For

the pressure dependence of the order parameter η , Eqs. (13) and (14) can be substituted into Eq. (4) at $T = T_1$ and $x = x_1$, which gives

$$\eta^2 = \eta_o^2 (P - P_1) \quad (17)$$

where $\eta_o^2 = a_{21}/a_{40}$. Using Eq. (17), the order parameter η was calculated as a function of pressure at constant temperatures and mole fractions, as indicated (Fig. 4) for the mixtures of n-tridecane (1) + n-hexane (1), n-hexadecane (1) + n-hexane (2) and n-octadecane (1) + n-hexane (2).

Similarly, for those three mixtures, the pressure dependence of the inverse susceptibility (χ_η^{-1}) was predicted at constant temperatures (and mole fractions), by means of Eq. (7). This was done by inserting Eq. (17) into Eq. (7) where the linear term in η was considered. Thus, the pressure dependence of the inverse susceptibility χ_η^{-1} is given by

$$\chi_\eta^{-1} = \chi_o^{-1} (P - P_1)^{1/2} \quad (18)$$

where the amplitude is defined as $\chi_o^{-1} = 4(a_{21}a_{40})^{1/2}$. χ_η^{-1} versus P plots are given in Fig. 4 for the mixtures of n-tridecane (1) + n-hexane (2), n-hexadecane (1) + n-hexane (2) and n-octadecane (1) + n-hexane (2).

Regarding the thermodynamic quantities of the heat capacity (C), entropy (S) and the enthalpy (H), those functions were also calculated as a function of pressure at constant temperatures (at constant mole fractions). By means of Eq. (15) at constant concentration (mole fraction, $x = x_1$), the pressure dependence of the heat capacity C through Eq. (8) is obtained as

$$C = C_o T [-\alpha_1 - \alpha_4 (P - P_1)]^{-1/2} \quad (19)$$

Also, the pressure dependence of the entropy difference $\Delta S = S - S_o$ can be expressed by using Eq. (9) in Eq. (15) as

$$\Delta S = \Delta S_o [-\alpha_1 - \alpha_4 (P - P_1)]^{1/2} \quad (20)$$

where $\Delta S_o = -2C_o$. The enthalpy difference $\Delta H = H - H_o$ which is given by Eq. (10), can be written as

$$\Delta H = \Delta H_o T [-\alpha_1 - \alpha_4 (P - P_1)]^{1/2} \quad (21)$$

with $H_o = -C_o$ by means of Eq. (15). Using Eqs. (19) - (21), respectively, for the solid – liquid transition in the mixtures studied as also indicated for the predictions of the order parameter and susceptibility. $C - P$, $S - P$ and $H - P$ plots at constant temperatures were predicted as given in Figs. (5-7), respectively. Those thermodynamic functions (C , ΔS and ΔH) were normalized. The α_0 and α_4 values of Eq. (15) (Tables 4 and 5) are also given for C , ΔS and ΔH functions in Table 6. On the basis of our assumptions for the coefficients a_2 (Eq. (13)) and a_4 (Eq. (14)), the pressure dependences of the order parameter η (Eq. (17)), the inverse susceptibility χ_η^{-1} (Eq. (18)), the heat capacity C (Eq. (19)), the entropy difference ΔS (Eq. (20)) and the enthalpy difference ΔH (Eq. (21)) were calculated for the solid – liquid transition in the binary mixtures studied. These dependences are also in accordance with the temperature dependences of

those functions based on our assumptions (a_2 and a_4) for the tetradecane + hexadecane as studied previously [23, 26].

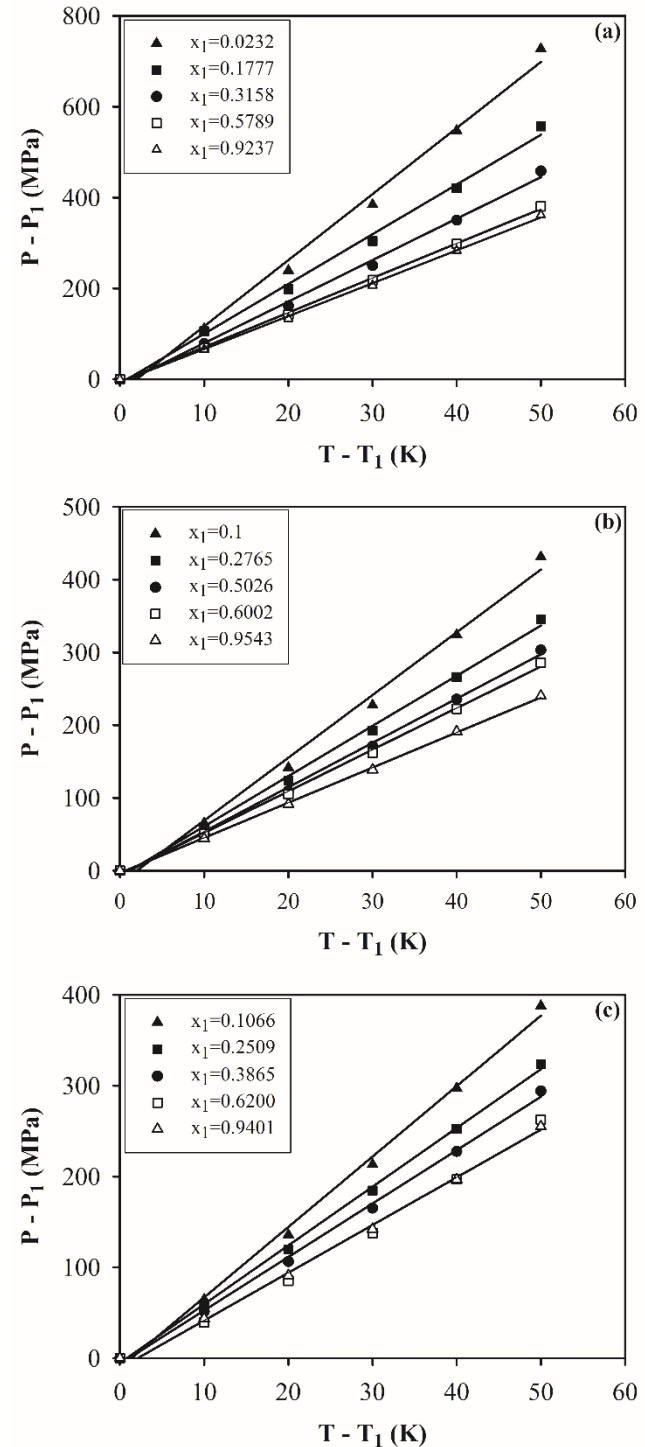


Figure 3. P - T phase diagrams calculated according to the phase line equation (Eq. (15)) which was fitted to the experimental data [32] for the solid – liquid transition of the mixtures a) n-tridecane (1) + n-hexane (2) b) n-hexadecane (1) + n-hexane (2) c) n-octadecane (1) + n-hexane (2) at constant mole fractions indicated. Experimental data are also shown in the figure.

This is because of the fact that the temperature T varies linearly with the pressure P for the binary mixtures studied here as measured experimentally [32]. In the case when T varies nonlinearly with the P , which can occur for some binary mixtures close to the solid – liquid transition, our assumption for the coefficient a_2 is no longer valid to

describe the $P - T$ phase diagram. However, the pressure dependence of η (Eq. (17)), χ_{η}^{-1} (Eq. (18)), C (Eq. (19)), ΔS (Eq. (20)) and ΔH (Eq. (21)) can still be used by ignoring some higher order terms to describe the solid - liquid transition in those binary mixtures.

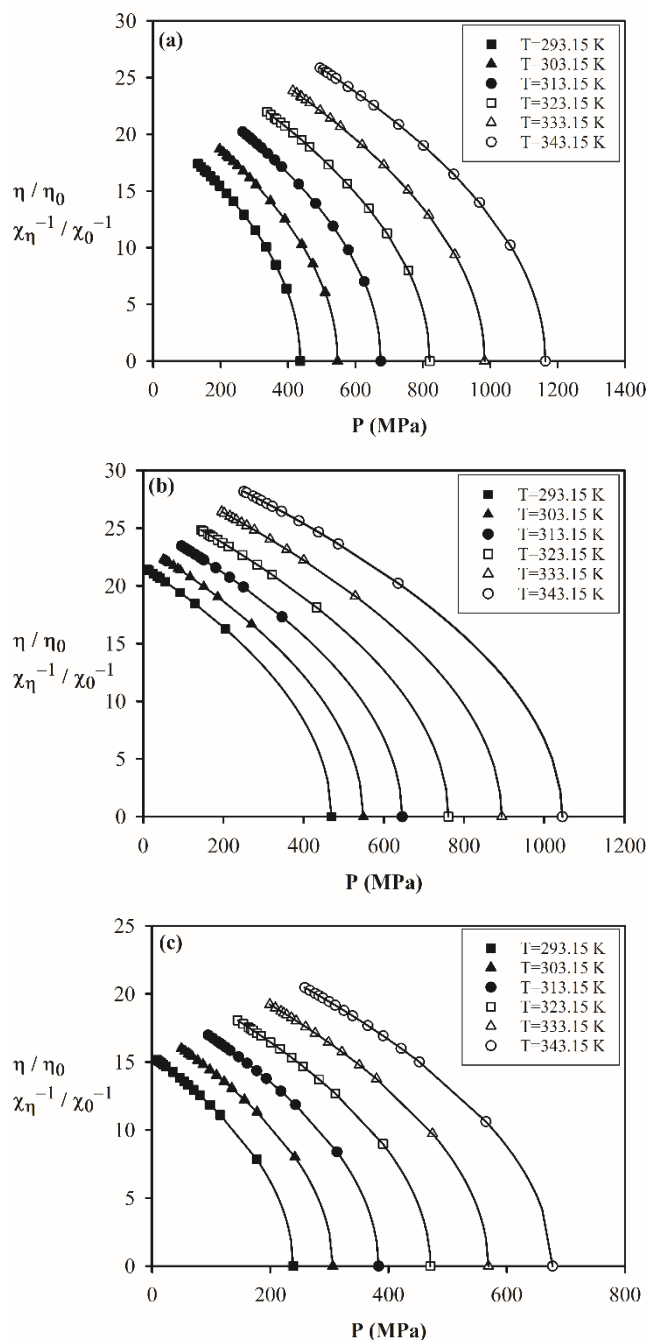


Figure 4. Pressure dependence of the order parameter η and the inverse susceptibility χ_{η}^{-1} (normalized) at constant temperatures within the experimental temperature intervals [32] according to Eqs. (17) and (18), respectively, for the solid - liquid transition in the mixtures a) *n*-tridecane (1) + *n*-hexane (2) b) *n*-hexadecane (1) + *n*-hexane (2) c) *n*-octadecane (1) + *n*-hexane (2).

4. Discussion

In this study, the temperature-concentration ($T - X$), the pressure-concentration ($P - X$) and the pressure-temperature ($P - T$) phase diagrams were described theoretically by the Landau mean field theory. Those phase diagrams involve the phase separation between the liquid and

solid phases. The Landau phenomenological model was used instead the Gibbs method of constructing of phase diagrams. Also, on this basis the thermodynamic functions of interest were calculated as a function of pressure for the binary mixtures studied, as stated above.

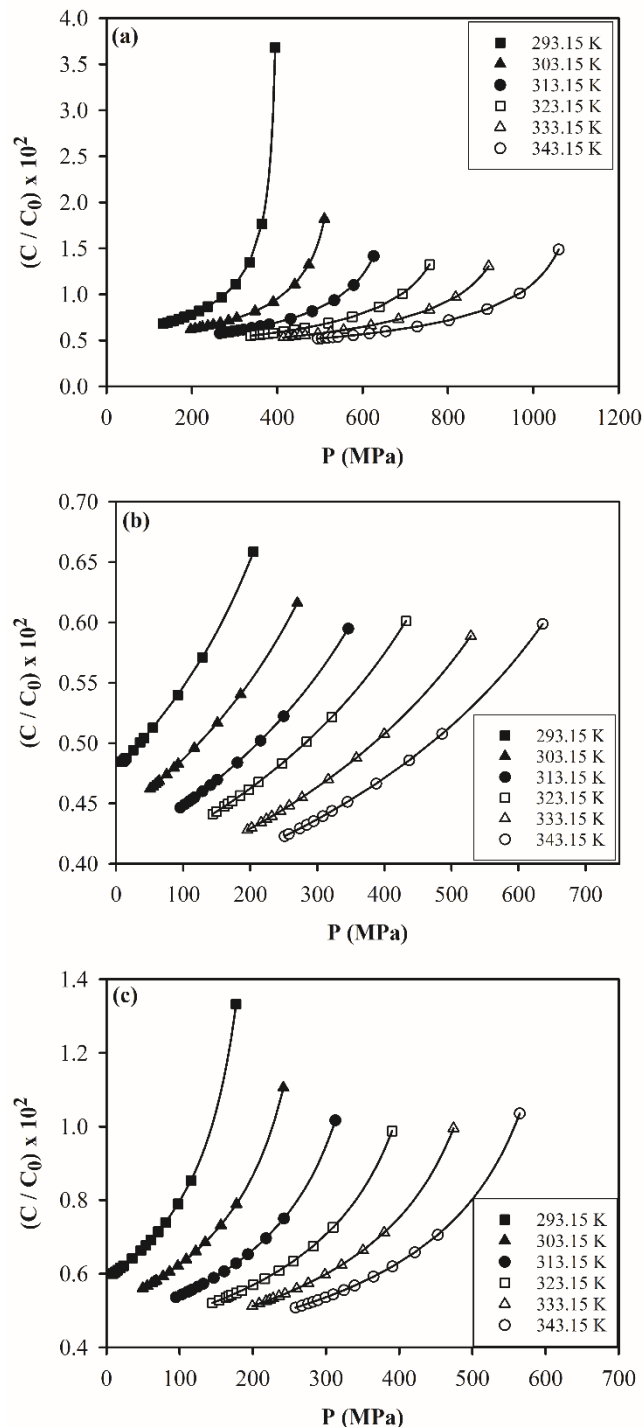


Figure 5. Pressure dependence of the heat capacity C at constant temperatures within the experimental temperature intervals [32] according to Eq. (19) for the solid - liquid transition in the mixtures a) *n*-tridecane (1) + *n*-hexane (2) b) *n*-hexadecane (1) + *n*-hexane (2) c) *n*-octadecane (1) + *n*-hexane (2).

$T - X$ phase diagrams of *n*-alkanes + *n*-cyclohexane at 300 MPa (Fig. 1), $P - X$ phase diagrams of *n*-alkanes + *n*-hexane at constant temperatures (Fig. 2) and $P - T$ phase diagrams of *n*-alkanes + *n*-hexane at constant concentrations (Fig. 3), which were obtained by fitting Eq. (15) to the

experimental data [32] are reasonably good. This shows that in the polynomial expansion (Eq. (15)), the cubic dependence of the concentration (mole fraction) on the temperature and pressure is adequate to describe the solid-liquid transition in those binary mixtures studied. This also confirms the functional form of the temperature and pressure dependence of the coefficient a_2 (Eq. (13)), and the concentration dependence of a_4 (Eq. (14)) for the phase line equation (Eq. (5)) in the expansion of the free energy F_s (Eq. (1)) which describes the solid-liquid transition in the binary mixtures of n-alkanes according to the Landau mean field theory. On the other hand, a linear dependence of some of the coefficients on the T and X variables to obtain, by a linear transformation, the phase diagram in the $T - X$ phase, has been assumed [39]. Also, a nonlinear dependence on concentration of the free energy coefficients has been considered for the liquid - solid transition to construct the temperature - concentration phase diagrams of binary eutectic mixtures [40], as was assumed in the present study. Another approach by representing an excess Gibbs energy model [41], the effect of pressure on the liquidus curve in a ($T - X$) phase diagram has been studied for the binary mixtures (tetradecane + pentadecane and tetradecane + hexadecane) [21]. By means of the Landau phenomenological model which explains the observed behaviour of the $T - X$ phase diagrams under pressure adequately, have been obtained for those binary mixtures in

our recent study [25]. This also shows that the Landau mean field model is satisfactory to obtain the $T - X$ phase diagram under high pressure, as we studied here for the binary mixtures of n-alkanes (1) + cyclohexane (2). As seen from the $T - X$ phase diagrams at 300 MPa (Fig. 1), the melting temperatures (T_1) increase with the small decrease in the composition x_1 of the cyclohexane for the n-alkanes namely, n-tridecane, n-hexadecane, n-octadecane and n-eicosane, respectively, on the basis of the experimental data [32]. Our $T - X$ phase diagrams (Fig. 1) show that the mixture of n-tridecane (1)+n-cyclohexane (2) is somehow different from the other three mixtures, namely, n-hexadecane, n-octadecane and n-eicosane, which follow almost the same phase line. This is mainly the variation of alkane molecule conformation and in -planar phase structure along with temperature. So that an increase in pressure can cause the composition and the structure of the different solid phases in this binary mixture. As noticed, the $T - T_1$ values of the n-tridecane are much lower than those three mixtures (Fig. 1). Similarly, as in the $T - X$ phase diagrams (Fig. 1), for the $P - X$ phase diagrams (Fig. 2) at constant temperatures, pressure increases as the concentration increases [32]. The melting pressure (P_1) increases as the temperature increases at a constant concentration (x_1) of n-hexane.

This is shown for example, at $x_1 = 0.0232$ (within the pressure range of 436.17 to 1163.74 MPa) for n-tridecane, $x_1 = 0.0260$ (pressure range of 469.45 to 1045.01 MPa) for

Table 5. Values of the coefficients determined for the solid - liquid transitions in the n-alkanes (1) + n-hexane (2) according to Eq. (15) which was fitted to the experimental data [32] at constant mole fractions indicated.

n-tridecane (1) + n-hexane (2)	x_1	0.0232	0.1777	0.3158	0.5789	0.9237
	α_0 (K)	2.159	0.967	1.391	0.764	0.881
	$\alpha_4 \times 10^{-2}$ (K/MPa)	6.82	9.09	10.91	13.12	13.79
n-hexadecane (1) + n-hexane (2)	x_1	0.1	0.2765	0.5026	0.6002	0.9543
	α_0 (K)	2.185	1.249	1.242	0.978	0.678
	α_4 (K/MPa)	0.115	0.144	0.164	0.175	0.207
n-octadecane (1) + n-hexane (2)	x_1	0.1066	0.2509	0.3865	0.6200	0.9401
	α_0 (K)	1.472	0.853	1.131	2.314	1.268
	α_4 (K/MPa)	0.128	0.154	0.170	0.189	0.196

Table 6. Values of the coefficients α_0 and α_4 according to Eq. (15) at $x = x_1$ for the n-alkanes (1) + n-hexane (2) as indicated at constant temperatures T_1 and pressure P_1 , which were determined to predict the pressure dependence of C (Fig. 5), S (Fig. 6) and H (Fig. 7).

n-tridecane (1) + n-hexane (2)	T_1 (K)	293.15	303.15	313.15	323.15	333.15	343.15
	$x_1 = 0.0232$						
	P_1 (MPa)	436.17	547.00	675.17	820.69	983.54	1163.74
$\alpha_4 = 6.821 \times 10^{-2}$ (K/MPa)	α_0 (K)	2.159	-0.282	-1.540	-1.614	-0.507	1.783
	n-hexadecane (1) + n-hexane (2)						
	P_1 (MPa)	469.45	548.68	645.85	760.97	894.02	1045.01
$x_1 = 0.0260$	α_0 (K)	2.884	-0.321	-1.199	-2.115	-0.705	2.244
	$\alpha_4 = 8.576 \times 10^{-2}$ (K/MPa)						
	P_1 (MPa)	238.60	305.71	383.16	470.94	569.05	677.49
n-octadecane (1) + n-hexane (2)	$x_1 = 0.0608$						
	α_0 (K)	2.131	-0.280	-1.521	-1.594	-0.499	1.764
	$\alpha_4 = 1.131 \times 10^{-2}$ (K/MPa)						

n-hexadecane and $x_1 = 0.0608$ (pressure range of 238.60 to 677.49 MPa) for n-octadecane on the basis of the experimental data [32].

From our $P - X$ phase diagrams (Fig. 2), we also see that the variation of $P_1 - P$ with the $x - x_1$ is rather smooth for the n-tridecane (Fig. 2a) as compared to those of n-hexadecane (Fig. 2b) and n-octadecane (Fig. 2c). So that for the n-tridecane (1) + n-hexane (2), the quadratic dependence of the concentration on the pressure, $P_1 - P \propto (x - x_1)^2$, according to Eq. (15) can also describe the observed data [32]. Since the cubic dependence of concentration on the pressure (Eq. 15) was fitted at constant temperatures to the $P - X$ phase diagrams of binary mixtures studied (Fig. 2), the best curve-fitting was obtained although some experimental data points [32] do not coincide with the curve exactly in Fig. 2b. Of course, it is always possible to fit the data perfectly by choosing different functional forms (higher order polynomials or exponential functions). However, this contradicts with the theory outlined and the method of calculation given in this study. One possible explanation is that the method of analysis is not well satisfied in the case of n-hexadecane (1) + n-hexane (2) (Fig. 2b) as compared to the binary mixtures of n-tridecane (1) + n-hexane (2) (Fig. 2a) and n-octadecane (1) + n-hexane (2) (Fig. 2c).

Note that the fourth order term was also considered in the concentration, $(x - x_1)^4$, in the expansion (Eq. (15)) to get the best fit for the $T - X$ phase diagram (Fig. 2b). But, this did not change the curve-fitting and some data points were not exactly on the curve as before (Fig. 2b). Regarding the $P - T$ phase diagrams of those binary mixtures of n-alkanes (Fig. 3), pressure increases as the temperature increases at constant compositions, as stated above. In our plots (Fig. 3), some constant concentrations of the n-hexane (1) were arbitrarily chosen for the binary mixtures of n-tridecane, n-hexadecane and n-octadecane by using the experimental data [32]. For the other constant compositions (x_1) between 0 and 1 as given from the experimental measurements [32] of those mixtures, the same behavior can be expected in the $P - T$ phase diagrams for their solid-liquid transitions. Note that the $T - P$ phase diagram for the high-pressure solid - liquid phase equilibria in synthetic waxes, in particular, melting curve of n-tridecane, has been obtained by the Landau mean field model using the experimental data [14], in our very recent study [27]. As indicated in the experimental study [14], the $T - P$ variation is not too far from linearity and the average slope between atmospheric and 100 MPa was estimated (0.193 K/MPa), which also confirms our linear $T - P$ assumption in our study [27] and the present study.

Note that increase in $T - T_1$ with the $x - x_1$ at 300 MPa as the concentration of n-alkanes (x_1) increases (Fig. 1) and also increase in $P - P_1$ with the $T - T_1$ at various concentrations (Fig. 3), occur above the melting point (T_1, P_1) for the solid - liquid transition in the binary mixtures studied. On the other hand, as the x_1 increases at constant temperatures, the pressure difference ($P_1 - P$) increases below the melting pressure (P_1) for the solid - liquid transition as given in Fig. 2. In terms of the binary mixtures studied, when n-cyclohexane (2) is concentrated with the n-alkanes (1), the freezing temperatures (T_1) of these binary mixture increase at a constant pressure (300 MPa) (Fig. 1), whereas the transition pressure (P_1) decreases at constant temperatures (Fig. 2) for the binary mixtures as measured experimentally [32]. At constant concentrations of the n-

alkane (1) + n-cyclohexane (2) increasing the freezing temperature (T_1) requires higher pressures (P_1) (Fig. 3).

For the $T - X$ (Fig. 1), $P - X$ (Fig. 2) and $P - T$ (Fig. 3) phase diagrams, Eq. (15) with the cubic dependence of the concentration and linear dependence of the pressure on the temperature, is adequate to describe the observed behaviour of the phase diagrams for the binary mixtures studied, as stated above. Initially, Eq. (15) was fitted to the experimental data [32] for all those mixtures separately with the curves covering all the experimental data points (Figs. 1-3). Our fittings showed us in the case of the binary mixtures n-hexadecane, n-octadecane and n-eicosane, their $T - X$ phase diagrams exhibited similar behaviour for the solid - liquid transition, which was different from the mixture of n-tridecane (Fig. 1). On that basis, a single curve was obtained for those binary mixtures as shown in Fig. 1. This is the reason why some data points are not exactly on the curve. Thus, this single curve characterizes the observed behaviour of those binary mixtures regarding their solid - liquid phase transition.

Note that instead of $T - X_1$, $P - X_1$ and $P - T$ plots for the binary mixtures as given experimentally [32], $T - T_1$ versus $x - x_1$ (Fig. 1), $P_1 - P$ versus $x - x_1$ (Fig. 2) and $P_1 - P$ versus $T - T_1$ (Fig. 3) were plotted according to Eq. (15) in our treatment. This provides variation of the temperature (with respect to the freezing temperature T_1) with the mole fraction x of n-alkane (1) at $P = 300 \text{ MPa}$ (Fig. 1), variation of the pressure (with respect to the transition pressure P_1) with the $(x - x_1)$ at constant temperatures (Fig. 2) and the variation of the $P - P_1$ with the $T - T_1$ at constant concentrations (Fig. 3), as stated above. In particular, in the case of the $T - T_1$ versus $x - x_1$ plot (Fig. 1), Eq. (15) was fitted to the experimental data [32] above $x_1 = 0.2$ up to $x_1 = 1.0$ for the n-alkane (1) + cyclohexane (2), where n-alkanes (1) are n-tridecane, n-hexadecane, n-octadecane and n-eicosane. Thus, the two discontinuous phase lines (above and below $x_1 = 0.2$) which coincide at the triple points for those binary mixtures do not appear in our $T - T_1$ versus $x - x_1$ plot (Fig. 1).

Also, in the case of the variation of $P - P_1$ with the $T - T_1$, at constant concentrations (Fig. 3), our fit is not reasonably well, in particular at $x_1 = 0.0232$ (Fig. 3a), $x_1 = 0.1$ (Fig. 3b) and $x_1 = 0.1066$ (Fig. 3c), as shown by the symbol \blacktriangle for the n-alkanes (1) + n-hexane (2). Our fits are good starting from the high concentrations ($x_1 \cong 0.92 - 0.95$) of the n-alkanes (1). As the constant concentration (x_1) decreases, regarding the variation of $P - P_1$ with the $T - T_1$, it seems that Eq. (15) does not describe the $T - X$ phase diagram satisfactorily. This would mean that the mean field model studied here, is probably inadequate to explain the observed $P - T$ phase diagram of the n-alkanes (1) + n-hexane (2) at very low concentrations (x_1).

On the basis of the phase diagrams ($T - X$, $P - X$ and $P - T$) for the binary mixtures of n-alkanes which were calculated, the pressure dependence of the order parameter, and susceptibility with the thermodynamic quantities of the heat capacity, entropy and enthalpy, were also predicted for the liquid-solid transition in those mixtures. According to Eq. (17), pressure dependence of the order parameter η (quadratic) from the Landau mean field theory, is satisfactory at constant temperatures for the n-alkanes (n-tridecane, hexadecane and n-octadecane) + n-hexane, as shown in Fig. 4. The order parameter η (normalized) decreases to zero as the transition pressure (P_1) is approached

at constant temperatures as indicated and it shifts to higher pressure values with increasing temperature (Fig. 4). The pressure dependence of the order parameter η (Eq. (17)) is the same as the temperature dependence of ψ (order parameter) (Eq. (12)) since the pressure ($P - P_1$) is directly proportional to the temperature ($T - T_1$) as shown for the binary mixtures (Fig. 3) on the basis of the experimental measurements [32]. Since the liquid phase has no ordering, the order parameter η of the solid phase goes to zero as the temperature increases to the melting temperature (T_1) or the pressure increases to the melting pressure (P_1) for the solid – liquid transition, as obtained for the binary mixtures studied (Fig. 4).

Considering the quadratic dependence of the order parameter η on the pressure (Eq. (17)) or its temperature dependence (Eq. (4)) through Eq. (13) with the critical exponent $1/2$ according to $\eta \propto (T - T_1)^{1/2}$, the transition can change its character from the first order to a second order or vice versa within the extended mean field model [34] when the order parameter is calculated from the heat capacity (Eq. (11)) according to Eq. (12) with the critical exponent $\phi = 1/4$. This indicates that the discontinuous (first order) change can become a continuous one (second order), which is tricritical transition with the critical exponent value $1/4$ of the order parameter within mean field theory [42, 43]. Experiments can examine the critical behavior of the order parameter as measured at various temperatures and pressures for the binary mixtures studied here.

Similarly, the pressure dependence of the inverse susceptibility (χ_η^{-1}) that was obtained for the mixtures of n-alkanes at constant temperatures (Fig. 4), exhibits the behavior as expected from the Landau phenomenological model according to Eq. (7) where the order parameter η (Eq. (17)) was used. Since the functional form of the inverse susceptibility of the order parameter as a function of the pressure (Eq. (18)) is the same as the order parameter η (Eq. (17)), it decreases with the pressure and it approaches to zero at the transition pressure (P_1) for those binary mixtures studied. That is why we plotted η (normalized) and χ_η^{-1} (normalized) as a function of pressure in the same figure (Fig. 4) for the solid – liquid transition in the binary mixtures studied. As in the case of the order parameter η (Fig. 4), the normalized inverse susceptibilities increase in their values as the temperature increases (Fig. 4). When the order parameter (η) and the inverse susceptibility (χ_η^{-1}) of the order parameter are normalized according to Eqs. (17) and (18), respectively, as a function of pressure at constant temperatures they characterize the same solid – liquid transition in the binary mixtures studied (Fig. 4), as stated above.

Since the melting pressure increases as the temperature increases (Fig. 3), the susceptibility χ_ψ (response function) of the order parameter, increasing with the temperature also increases (or the inverse susceptibility decreases) with the pressure at constant temperatures. This occurs at constant temperatures from 293.15 to 343.15 K, accompanied with the increasing the melting pressure. This is shown also in the inverse susceptibility as the order parameter for the solid – liquid transition in the mixtures studied (Fig. 4). Note that for the variation of χ_η^{-1} with the pressure, only the linear term in η was considered with the critical exponent $1/2$ of η (Eq. (17)), which is the dominant term as compared to the η^3 term (Eq. (7)) with the exponent $3/2$.

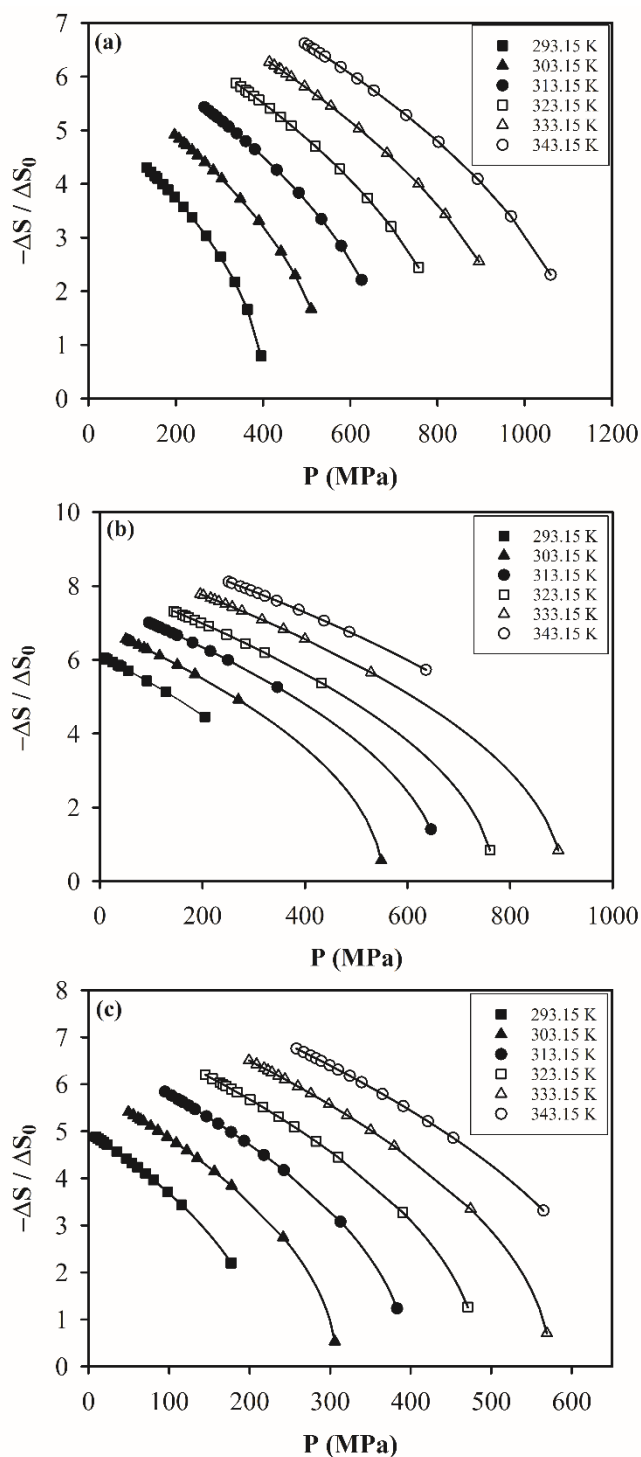


Figure 6. Pressure dependence of the entropy difference ΔS at constant temperatures within the experimental temperature intervals [32] according to Eq. (20) for the solid – liquid transition in the mixtures a) n-tridecane (1) + n-hexane (2) b) n-hexadecane (1) + n-hexane (2) c) n-octadecane (1) + n-hexane (2). ΔS is normalized ($\Delta S/\Delta S_0$) where $\Delta S_0 = 2C_0$ (Eq. (20)).

Regarding the thermodynamic quantities of the heat capacity (C), entropy (S) and the enthalpy (H), the extended mean field model [34] was employed according to Eqs. (8), (9) and (10), respectively, as stated above. The pressure dependence of the heat capacity which was calculated by means of Eq. (19), shows divergence behaviour with the critical exponent $\alpha = 1/2$, as expected from the extended mean field model [34]. This occurred at constant temperatures from 293.15 K to 343.15 K for the binary

mixtures of n-tridecane + n-hexane, n-hexadecane + n-hexane and n-octadecane + n-hexane (Fig. 5). As seen from this figure, variation of the heat capacity C (normalized) is considerably sharp with the pressure at 293.15 K as compared to the other constant temperatures for n-tridecane (Fig. 5a). Also, its magnitude is higher at this temperature ($T = 293.15\text{ K}$) in comparison with those at the other temperatures for all the three mixtures (Fig. 5).

It can be considered that in a very small temperature interval close to the freezing temperature T_1 , the heat capacity (C) diverges largely as a function of temperature at zero pressure ($P = 0$) according to Eq. (8) for the liquid – solid transition. Correspondingly, a large divergence behaviour of the heat capacity can occur in a very small pressure interval close to the transition pressure P_1 as a function of pressure at the room temperature ($T = 293.15\text{ K}$) under the experimental conditions ($P = 0$, $T = 293.15\text{ K}$) according to Eq. (19) for the liquid – solid transition. This is a possible explanation why the critical behaviour of the heat capacity (C) as a function of pressure at 293.15 K, is different from those at higher temperatures for the solid – liquid transition in the n-alkanes (1) + n-hexane (2) mixtures (Fig. 5). We see that the heat capacity (C/C_0) increases smoothly with the increasing pressure (except at 293.15 K) at the constant temperatures indicated for those binary mixtures as studied here (Fig. 5). Pressure dependence of the heat capacity exhibits similar critical behavior for those three mixtures close to their liquid-solid transition according to the extended mean field model which can be examined experimentally for those binary mixtures.

On the basis of the critical behavior of the heat capacity (C) at various pressures for constant temperatures (Fig. 5), the entropy difference ΔS and the enthalpy difference ΔH are also expected to exhibit similar behavior with the pressure (at constant temperatures), according to Eqs. (20) and (21), which are shown in Figs. 6 and 7, respectively, for the three binary mixtures, namely, n-tridecane + n-hexane, n-hexadecane + n-hexane and n-octadecane + n-hexane close to their solid-liquid transition.

This is due to the fact that the pressure dependences of the ΔS (normalized) and ΔH (normalized) are in the same functional form except that ΔH is divided by the temperature T (constant), as given by Eqs. (20) and (21), which were plotted in Figs. (6) and (7), respectively. Since both functions (ΔS and ΔH) were derived from the heat capacity C , their temperature (Eqs. (9) and (10)) or pressure (Eqs. (20) and (21)) dependences exhibit within the extended mean field model [34] similar solid – liquid transition for the binary mixtures studied. This was exemplified for the order parameter η and the inverse susceptibility χ_ψ^{-1} (Fig. 4) also in the present study. Note that similar to our treatment, entropy and enthalpy were calculated based on the heat capacity curve fitting for the experimental measurements of n-alkanes in a wide temperature range from 1.9 K to 370 K using differential scanning and adiabatic calorimetry method [36]. As indicated in our previous study [21], the difference in the enthalpy ΔH as the observed heat of fusion, increases with increasing temperature, which was observed experimentally for the tetradecane + hexadecane. Since T is directly proportional to the pressure as assumed here (Eq. (15)) with the $P - T$ phase diagrams (Fig. 3) for the binary mixtures studied here, enthalpy (ΔH) should be increasing with the pressure (or negative ΔH decreases with P), as given in Fig. 7 for those binary mixtures.

Similar behaviour of the ΔS and ΔH due to the critical behaviour of the heat capacity from the extended mean field model [34] which can be tested by the measurements of those quantities for the solid-liquid transitions of the binary mixtures as studied here.

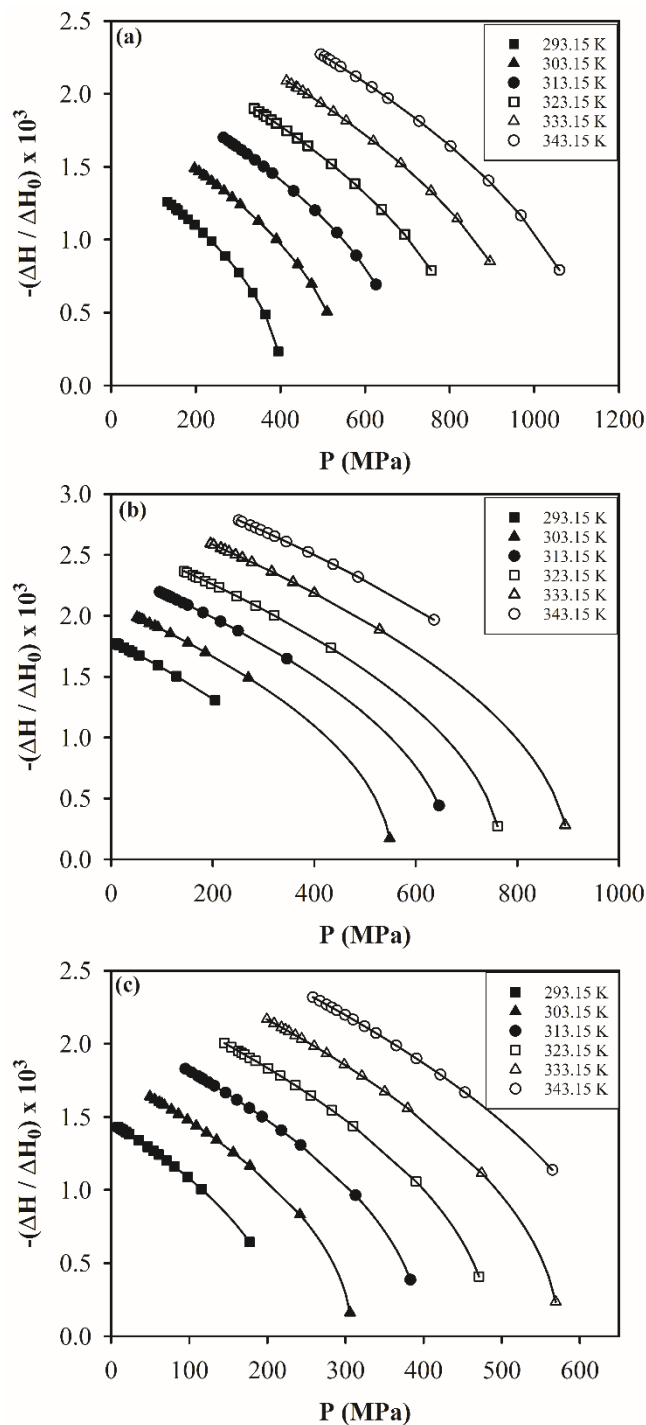


Figure 7. Pressure dependence of the difference ΔH at constant temperatures within the experimental temperature intervals [32] according to Eq. (21) for the solid – liquid transition in the mixtures a) n-tridecane (1) + n-hexane (2) b) n-hexadecane (1) + n-hexane (2) c) n-octadecane (1) + n-hexane (2). ΔH is normalized ($\Delta H / \Delta H_0$) where $\Delta H_0 = C_0$ (Eq. (21)).

5. Conclusions

The free energy of the solid phase was expanded in terms of the solid phase under pressure for the solid – liquid transition in the binary mixtures of n-alkanes within the

framework of the Landau phenomenological model. The $T - X$ (at 300 MPa), $P - X$ (at constant temperatures) and $P - T$ (at constant concentrations) phase diagrams were obtained for those binary mixtures by using the experimental data from the literature. Cubic dependence of the concentration on the temperature ($T - X$) and the linear dependence of the pressure on the temperature ($P - T$) were considered in our treatment. The $T - X$ phase diagram of n-alkanes (1) (n-hexadecane, n-octadecane and n-eicosane) + cyclohexane (2) was represented by a single non-linear curve, whereas for the n-tridecane (1) + cyclohexane (2) T varied almost linearly with x . The pressure dependences of the order parameter, susceptibility, heat capacity, entropy and the enthalpy, were also predicted for the mixtures studied. Those predictions studied as a function of pressure can be tested experimentally for the binary mixtures at constant temperatures and concentrations. This can explain the pressure effect on the phase diagrams and on the thermodynamic functions to describe the mechanism of the solid – liquid transition in the binary mixtures for future studies.

Nomenclature

T	temperature (K)
T_1	melting temperature (K)
x	concentration (mole fraction) (%)
x_1	melting concentration (%)
P	pressure (MPa)
P_1	melting pressure (MPa)
η	order parameter
χ_η	order parameter susceptibility
F	free energy (J/mol)
C, C_0	heat capacity (J/mol.K)
S, S_0	entropy (J/mol.K)
H, H_0	enthalpy (J/mol)

References:

- [1] D.S. Fu, Y.L. Su, B.Q. Xie, H.J. Zhu, G.M. Liu and D.J. Wang, “Phase change materials of n-alkane-containing microcapsules: observation of coexistence of ordered and rotator phases”, *Phys. Chem. Chem. Phys.*, *13*, 2021-2026, 2011.
- [2] D.S. Fu, Y.F. Liu, X. Gao, Y.L. Su, G.M. Liu, D.J. Wang, “Binary n-Alkane Mixtures from Total Miscibility to Phase Separation in Microcapsules: Enrichment of Shorter Component in Surface Freezing and Enhanced Stability of Rotator Phases”, *J. Phys. Chem. B*, *116*, 3099-3105, 2012.
- [3] P.K. Mukherjee, “Pressure effect on the rotator-II to rotator I transition of alkanes”, *J. Chem. Phys.*, *130*, 214906, 2009.
- [4] A. Craievich, J. Doucet and I. Denicolo, “Molecular disorder in even-numbered paraffins”, *Phys. Rev. B*, *32*, 4164-4168, 1985.
- [5] G. Ungar, N. Masic, “Order in the rotator phase of normal alkanes”, *J. Phys. Chem.*, *89*, 1036-1042, 1985.
- [6] E. B. Sirota, “Rotator phases of the normal alkanes: An x-ray scattering study”, *J. Chem. Phys.*, *98*, 5809-5824, 1993.
- [7] E. B. Sirota, “Remarks concerning the relation between rotator phases of bulk n-alkanes and those of langmuir

monolayers of alkyl-chain surfactants on water”, *Langmuir*, *13*, 3849-3859, 1997.

- [8] I. Koljanin, M. Pozar, B. Lovrinevic, “Structure and Dynamics of liquid linear and cyclic alkanes: A molecular Dynamics study”, *Fluid Phase Equilibria*, *550*, 113237, 2021.
- [9] D.S. Fu, Y.F. Liu, G.M. Liu, Y.L. Su, D.J. Wang, “Confined crystallization of binary n-alkane mixtures: stabilization of a new rotator phase by enhanced surface freezing and weakened intermolecular interactions”, *Phys. Chem. Chem. Phys.*, *13*, 15031-15036, 2011.
- [10] R.R. Nelson, W. Webb and J.A. Dixon, “First-order phase transitions of six normal paraffins at elevated pressures”, *J. Chem. Phys.*, *33*, 1756-1764, 1960.
- [11] B. Koppitz and A. Würflinger, “Differential thermal analysis at elevated pressure”, *Colloid Polym. Sci.*, *252*, 999-1000, 1974.
- [12] C. Josefiak, A. Würflinger and G.M. Schneider, “Differential thermal analysis under high pressure”, *Colloid Polym. Sci.*, *255*, 170-171, 1977.
- [13] S.N. Gunasekara, S. Kumova, J.N. Chiu, V. Martin, “Experimental phase diagram of the dodecane-tridecane system as phase change material in cold storage”, *Int. J. Ref.*, *82*, 130-140, 2017.
- [14] J.L. Daridon, J. Pauly and M. Milhet, “High pressure solid-liquid phase equilibria in synthetic waxes”, *Phys. Chem. Chem. Phys.*, *4*, 4458-4461, 2002.
- [15] T. Shen, H. Peng, X. Ling, “Experimental Measurements and Thermodynamic Modeling of Melting Temperature of the Binary Systems n-C11H24-n-C14H30, n-C12H26-n-C13H28, n-C12H26-n-C14H30, and n-C13H28-n-C-15 H-32 for Cryogenic Thermal Energy Storage”, *Ind. Eng. Chem. Res.*, *58*, 15026-15035, 2019.
- [16] P.K. Mukherjee and M. Deutsch, “Landau theory of the R-II-R-I-R-V rotator phases of alkanes”, *Phys. Rev. B*, *60*, 3154-3162, 1999.
- [17] C. Ma, Q. Zhou, F. Li, J. Hao, J. Wang, L. Huang, F. Huang, Q. Cui, “Rotator phases of n-heptane under high pressure: Raman scattering and X-ray diffraction studies”, *J. Phys. Chem. C*, *115*, 18310-18345, 2011.
- [18] M. Krishnan, S. Balasubramanian, “n-heptane under pressure: Structure and dynamics from molecular simulations”, *J. Phys. Chem. B*, *109*, 1936-1946, 2005.
- [19] D. Cholakov and N. Denkov, “Rotator phases in alkane systems: In bulk, surface layers and micro/nano-confinements”, *Adv. Colloid Interface Sci.*, *269*, 7-42, 2019.
- [20] B. He, V. Martin, F. Setterwall, “Liquid-solid phase equilibrium study of tetradecane and hexadecane binary mixtures as phase change materials (PCMs) for comfort cooling storage”, *Fluid Phase Equilibria*, *212*, 97-109, 2003.
- [21] M. Milhet, J. Pauly, J.A.P. Coutinho, M. Dirand, J.L. Daridon, “Liquid-solid equilibria under high pressure of tetradecane plus pentadecane and tetradecane plus hexadecane binary systems”, *Fluid Phase Equilibria*, *235*, 173-181, 2005.

- [22] S. Corsetti, T. Rabl, D. McGloin and J. Kiefer, "Intermediate phases during solid to liquid transitions in long-chain n-alkanes", *Phys. Chem. Chem. Phys.*, *19*, 13941-13950, 2017.
- [23] H. Yurtseven, T. Emirosmanglu, O. Tari, "Calculation of the Liquid-Solid Phase Diagram and the Thermodynamic Quantities of the Binary System of Tetradecane and Hexadecane Using the Mean Field Theory", *J. Sol. Chem.*, *50*, 1335-1362, 2021.
- [24] H. Yurtseven, E. Kilit Dogan, "Calculation of the phase diagram of n-alkanes (C_nH_{2n+2}) by the Landau mean field theory", *Fluid Phase Equilibria*, *556*, 113377, 2022.
- [25] O. Tari, H. Yurtseven, "Calculation of the T-X phase diagram of tetradecane+hexadecane and tetradecane+pentadecane under high pressure by the Landau mean field theory", *Fluid Phase Equilibria*, *559*, 113499, 2022.
- [26] H. Yurtseven and O. Tari, "Calculation of the T-X phase diagram and the thermodynamic quantities for the binary mixtures of tetradecane + hexadecane using the Landau mean field model", *Phys. Chem. Liq.*, *61*, 340-364, 2023.
- [27] O. Tari and H. Yurtseven, "Calculation of the phase diagrams (T - X and T - P) and the thermodynamic quantities for the solid - liquid equilibria in n-tridecane", *Int. J. Thermodynamics*, *26*, 37-45, 2023.
- [28] H. Yan, H. Yang, J. Luo, N. Yin, Z. Tan and Q. Shi, "Thermodynamic insights into n-alkanes phase change materials for thermal energy storage", *Chin. Chem. Lett.*, *32*, 3825-3832, 2021.
- [29] S. A. Burrows, I. Korotkin, S.K. Smoukov, E. Boek and S. Karabasov, "Benchmarking of Molecular Dynamics Force Fields for Solid-Liquid and Solid-Solid Phase Transitions in Alkanes", *J. Phys. Chem. B*, *125*, 5145-5159, 2021.
- [30] P.K. Mukherjee, "Effect of silica nanoparticles on the heat capacity of the rotator phase transitions of alkanes", *Phase Transit.*, *95*, 322-330, 2022.
- [31] D. Cholakova, D. Glushkova, Z. Valkova, S. Tsibranska-Gyoreva, K. Tsvetkova, S. Tcholakova and N. Denkov, "Rotator phases in hexadecane emulsion drops revealed by X-ray synchrotron techniques", *J. Colloid Interface Sci.*, *604*, 260-271, 2021.
- [32] P. Morawski, J. A. P. Coutinho, U. Domanska, "High pressure (solid + liquid) equilibria of n-alkane mixtures: experimental results, correlation and prediction", *Fluid Phase Equilibria*, *230*, 72-80, 2005.
- [33] G. Fritsch, "A Landau-type model for the melting transition", *Phys. Stat. Sol. (a)*, *31*, 107-118, 1975.
- [34] C.C. Huang and J.M. Viner, "Nature of the Smectic-A-Smectic-C phase transition in liquid crystals", *Phys. Rev. A*, *25*, 3385-3388, 1982.
- [35] S. Dumrongrattana, G. Nounesis and C.C. Huang, "Measurement of tilt angle and heat capacity in the vicinity of one smectic-A chiral smectic-C transition", *Phys. Rev. A*, *33*, 2181-2183, 1986.
- [36] P.K. Mukherjee, "Simple Landau model of the RIV-RIII-RV rotator phases of alkanes", *J. Chem. Phys.*, *129*, 021101, 2008.
- [37] P.K. Mukherjee, "Tricritical behavior of the RI-RV rotator phase transition in a mixture of alkanes with nanoparticles", *J. Chem. Phys.*, *135*, 134505, 2011.
- [38] P.K. Mukherjee and S. Dey, "Simple Landau Model of the Liquid-RII-RI Rotator Phases of Alkanes". *J. Mod. Phys.*, *3*, 80-84, 2012.
- [39] J.C. Toledano and P. Toledano, "The Landau theory of Phase Transition", World Scientific, Singapore, 1987.
- [40] D. Machon, "Phenomenological theory of the phase diagrams of binary eutectic systems", *Phys. Rev. B*, *71*, 024110, 2005.
- [41] A. Hammami and M. Raines, "Paraffin deposition from crude oils: comparison of laboratory results to field data", *SPE-38776*, 273-287, 1997.
- [42] H. E. Stanley, *Introduction to Phase Transitions and Critical Phenomena*, Clarendon, Oxford, 1971.
- [43] J.J. Binner, N. J. Dowrick, A. J. Fisher, M.E.J. Newman, *The Theory of Critical Phenomena, An Introduction to the Renormalization Group*, Oxford University Press, New York, Chapter 3, 1992.